Journal of the Brazilian Society of Mechanical Sciences and Engineering (2019) 41:451
https://doi.org/10.1007/s40430-019-1948-8

TECHNICAL PAPER

Effect of different machining parameters on surface roughness of aluminium alloys based on Si and Mg content

Taoheed Olohunde Sadiq[1,2] · Baloch Abdul Hameed[1] · Jamaliah Idris[1] · Olusegun Olaoye[3] · Siti Nursyaza[1] · Zul Hairi Samsudin[1] · Mohamad Imran Hasnan[1]

Received: 30 March 2019 / Accepted: 9 September 2019 / Published online: 23 September 2019

Abstract
Aluminium-based alloys are considered lengthily for many applications in engineering areas due to their good mechanical properties. Machining these alloys had attracted the attention of many researchers on how to improve the machining, especially when high manufacturing rate is demanded. Usually, machining these materials poses some difficulties such as burr formation, roughness of the surface, continuous chip formation and build-up edge on cutting edge. In this study, AA6061T6, LM6 and AA5083 aluminium-based alloys were considered to research the optimum drilling parameters with the aim to address the earlier started challenges. Drillings were carried out by using a MAHO three-axis CNC drilling machine with an HSS drilling bit at three different spindle speeds and feed rates. From the results, it was established that each aluminium alloy has different surface roughnesses and this surface roughness decreases as spindle speeds increased. A minimum build-up edge was achieved for AA5083 and AA6061T6 alloys. However, a relatively high BUE was noticed in LM6.

Keywords Aluminium alloys · Surface roughness · Chip morphology · Build-up edge · Drilling parameters

1 Introduction

The applications of aluminium-based alloys are attracted by many companies such as aerospace, train and automotive industries because they serve as alternatives to the steel and cast iron parts due to their lightness and high strength [1, 2]. They possessed weight saving which reduces the fuel burning up and environmental influence. The sixth (6xxx) series, fifth (5xxx) and LM6 aluminium alloys have many important features such as medium strength, formability, weldability, corrosion resistance and low cost [3]. The A6061 hardening alloy composed magnesium, aluminium and silicon as the main chemical compositions. Due to the distinguishable mechanical properties, this material is abundantly required for various applications in aerospace and automotive industries [4, 5]. A6061 aluminium alloy is widely accepted in manufacturing lightweight shapes that demand a good corrosion resistance and a particular strength [6]. This aluminium alloy is also extensively used in fabricating pipes and storage tanks [6]. A5083 is another aluminium-based alloy; it possesses many

Technical Editor: Adriano Fagali de Souza.

✉ Jamaliah Idris
jamaliah@mail.fkm.utm.my

Taoheed Olohunde Sadiq
adisaolohunde@yahoo.com

Baloch Abdul Hameed
rawkhail@yahoo.com

Olusegun Olaoye
olaoyeos@gmail.com

Siti Nursyaza
syazamisran@yahoo.com

Zul Hairi Samsudin
zhs.25.joule@gmail.com

Mohamad Imran Hasnan
mohamad.imran.hasnan@gmail.com

[1] School of Engineering, Faculty of Mechanical Engineering, Universiti Teknologi Malaysia, 81310 Skudai, Johor Bahru, Malaysia

[2] Manufacturing Department, Engineering Materials Development Institute, KM4, Ondo Road, P.M.B 611, Akure, Ondo State, Nigeria

[3] Department of Mechanical Engineering, Ladoke Akintola University of Technology, Ogbomoso, Oyo State, Nigeria

distinguishable features, e.g. formability with super-plasticity, good strength, low price and good corrosion resistance [7]. The automobile industry is attracted by these good advantages of A5083 alloy; it is used to manufacture vehicles with good fuel efficiency [7]. Also, A5083 alloy material is considered for ships and crafts components due its good resistance [8]. LM6 aluminium alloy is an aluminium material produced by casting; it is generally considered for many structural applications in automobile and manufacturing industries [9].

Recently, the strength of aluminium-based materials has been enhanced meaningfully by adding titanium (Ti), magnesium (Mg), lithium (Li) and copper (Cu) as alloying elements [10]. The Mg_2Si intermetallic bonded material is strengthened by in situ in aluminium-built composites which possessed high hardness, low density, high elastic modulus, high melting temperature and low thermal expansion coefficient. However, rough eutectic and primary Mg_2Si phases cause weak mechanical properties. With the advancement in technological productions, attempts are made to adopt a close net figure from these alloy-based materials, but it requires some quality of finishing to accomplish the assembly procedure [11]. Consequently, it is vital to obtain optimal parameters for machining different aluminium (Mg and Si) alloys with different values of hardness; this would improve the production rates and give a better surface roughness. This is necessary because it would provide more useful information about the optimum machining parameters for a better surface roughness of A6061T6, LM6 and A5083 containing different weight per cents of Si and Mg.

Silicon (Si) is identified as important alloying element usually used to improve the fluidity of molten metal for sound castings; it also aids high hardness and strength of aluminium alloys. However, the increase in silicon content may lead to wearing of the tool during material ejection while dealing Al alloy castings. Likewise, magnesium (Mg) content is also important and desirable in aluminium alloys; it improves their hardness and strength. It is vital to compare the surface roughness for the aluminium-based alloys selected by using different machining parameters based on their different weight percentages of Si and Mg content to achieve acceptable chip forms and improved drill holes in terms of surface roughness.

Therefore, this study is concerned to establish a comparison of very basic optimized machining parameters for these alloys by performing drilling operations for surface roughness.

2 Sample preparation and experimental techniques

2.1 Casting procedure

Two kilograms of each wrought aluminium alloy A6061, A5083 and LM6 was weighted, and they were cleaned with acetone and deionised water to remove any conceivable dirt [12]. Thereafter, each alloy was melted in an electric induction furnace in a SiC crucible. The alloys were heated at a pouring temperature of 700 ± 10 °C. Then, the molten alloy was poured into a cast iron mould preheated at 200 °C in an electrical heating furnace and allowed to solidify at ambient temperature [13]. After the solidification and cooling down to room temperature, the mould was opened and the casting was taken out. Later, the remaining riser, gate and sprue were cut out using hand saw. The melting and pouring temperature was repeated for each sample. Preliminary machining was done to remove the burrs and reduce surface contaminant of the material on a milling machine, and the final dimension of the blocks was set 200 mm × 60 mm × 30 mm.

2.2 T6 heat treatment

A6061 aluminium alloy sample was solutionized and artificially aged. The sample block was kept in an auto-controlled heating furnace already heated at a fixed temperature of 600 °C for 3 h [5]. After the heat treatment, the sample was carefully taken out from the furnace and quenched in tap water. The sample was artificially aged by leaving it at room temperature for 3 h and then kept in an electric oven preheated at a temperature of 200 °C for 10 h [4]. Thereafter, the sample was taken out and water quenched.

2.3 Metallography

To reveal the particular structure of the samples by metallographic process, specimens were cut from each alloy and were grinded with SiC sand paper, followed by the fine series of grit sizes from 240 to 4000 µm. Then, the specimens were subjected to a final polishing with polishing cloth and alumina until a scratch-free mirror finish was obtained. After that, the alloys were etched in a solution of 95% water and 5% HF. The microstructure of the started samples was studied by an Olympus optical microscope (BX60F5) and scanning electron microscope inbuilt with energy-dispersive spectroscope.

2.4 CNC drilling

MAHO CNC drilling machine was used to perform the drilling operations. The machining parameters were selected to drill each sample and to know the optimum machining parameters for each alloy in terms of surface

Table 1 Drilling parameters

Machining parameter	Range of spindle speed and feed rate		
Spindle speed (rpm)	1000	2000	3000
Feed rate (mm/rev)	0.05	0.1	0.15

Table 2 Arrangement of experiments on each sample

Number of experiments								
1	2	3	4	5	6	7	8	9
N1f1 (1000), (50)	N1f2 1000), (100)	N1f3 (1000), (150)	N2f1 (2000), (50)	N2f2 (2000), (100)	N2f3 (2000), (150)	N3f1 (3000), (50)	N3f2 (3000), (100)	N3f3 (3000), (150)

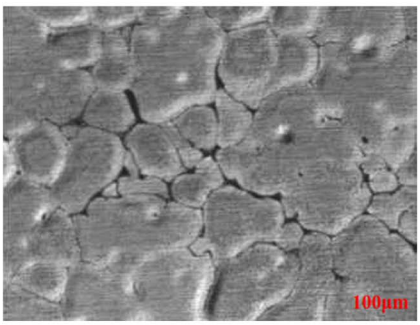

(a) Microstructural image of A6061T6 sample

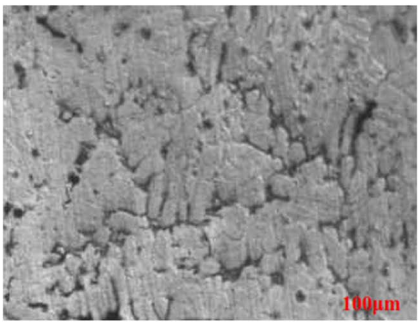

(b) Microstructural image of A5083 sample

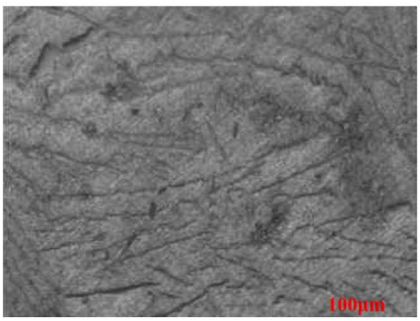

(c) Microstructural image of LM6 sample

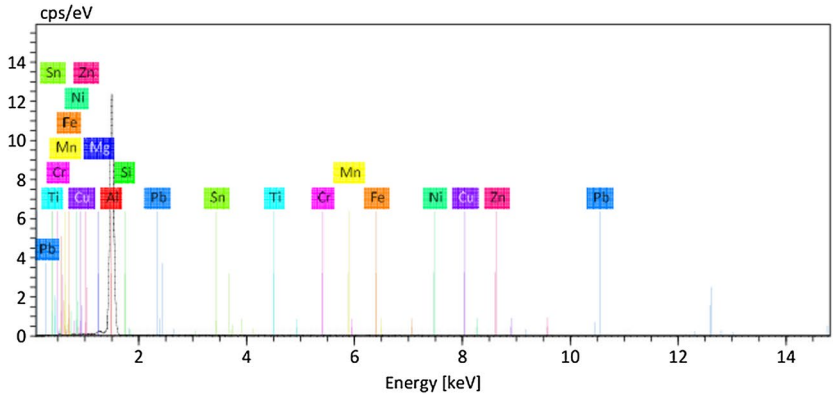

(d) EDS spectrum of A6061T6 sample

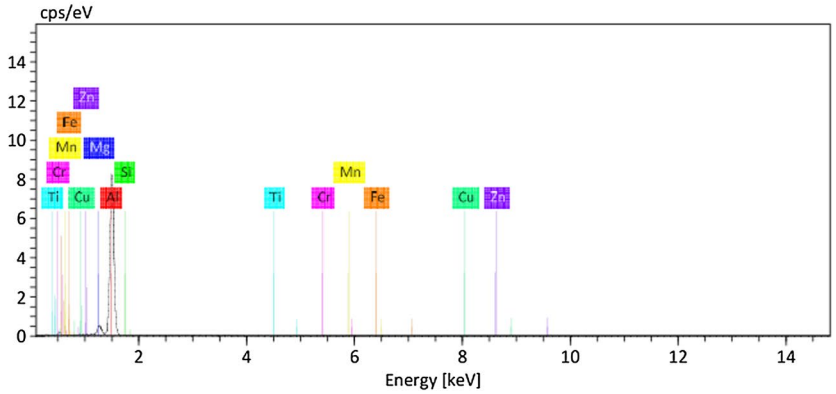

(e) EDS pattern of A5083 sample

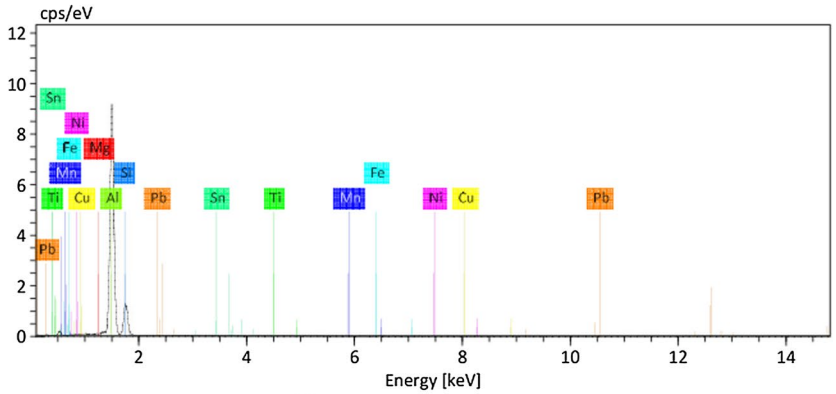

(f) EDS image of LM6 sample

Fig. 1 **a** Microstructural image of A6061T6 sample, **b** microstructural image of A5083 sample, **c** microstructural image of LM6 sample, **d** EDS spectrum of A6061T6 sample, **e**: EDS pattern of A5083 sample, **f**: EDS image of LM6 sample

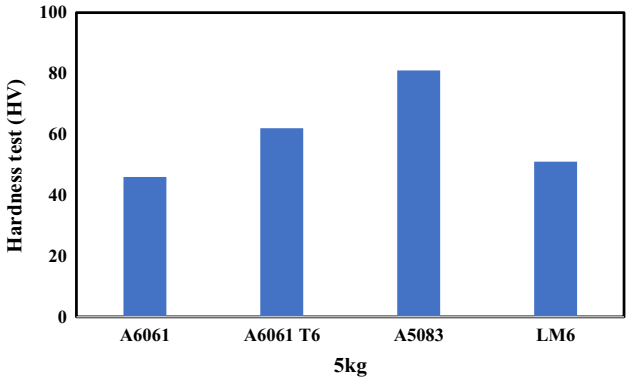

Fig. 2 Hardness test of the samples

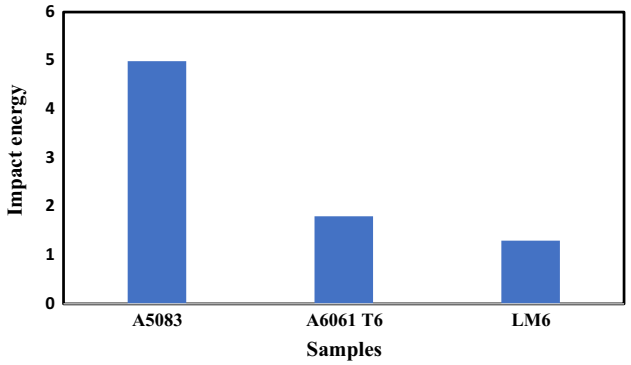

Fig. 3 Energy absorbed during impact test

Table 3 The surface roughness values for each sample with different drilling parameters

Number of experiments	Material surface roughness (μm)		
	LM6	A5083	A6061 T6
01	10.4	5.4	6.2
02	8.8	7.5	5.8
03	8.4	5.1	4.8
04	6.8	7.2	6.0
05	8.2	7.6	5.8
06	6.8	6.2	6.6
07	8.6	6.4	6.0
08	8.0	6.2	6.2
09	5.1	8.1	4.4

roughness, burr height, build-up edge, chip morphology and accuracy of hole. The different machining parameters used are shown in Table 1. Nine experiments were performed on each sample, and each hole was produced with a set of three same spindle speeds but different feed rates by using an HSS twist drill. The procedural arrangement for

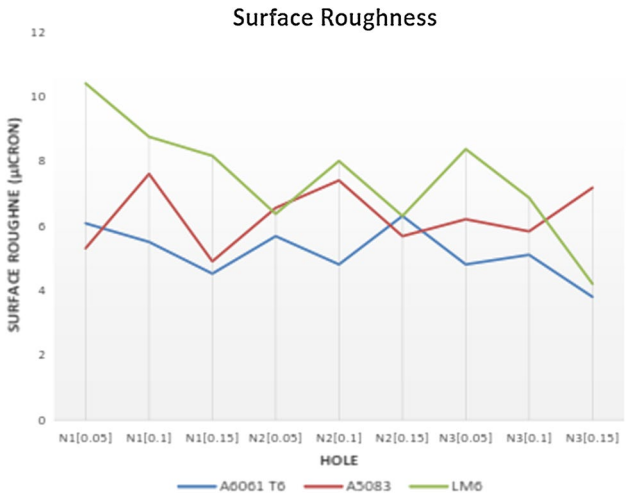

Fig. 4 Surface roughness values for each sample

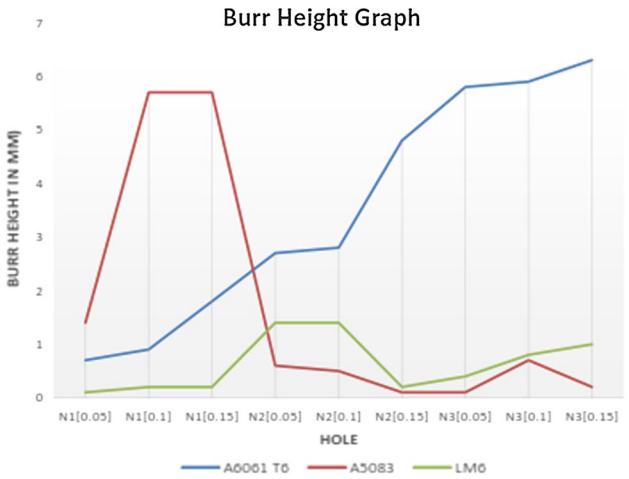

Fig. 5 Formation of burrs at each hole for each sample

each experiment on each sample as presented in Table 2 was dully followed.

Let the total number of experiments on each sample be equal to X.

Then,

X = (N1, N2, N3) (f1, f2,f3) OR

X = N1f1, N1f2, N1f3; N2f1, N2f2, N2f3; N3f1, N3f2, N3f3

X = 9 experiments

2.5 Other operations and tests

The surface roughness was measured with a surface profilometer at four different locations at a relative angle of 90°. For repeatability of the test, each measurement was repeated twice. Vickers hardness testing machine was used

to measure the hardness of each sample. A load of 5 kg was applied at a rate of 100 µm/s for a dwell time of 20 s. Five measurements were taken, and the average was calculated. This was repeated for each sample.

For the chip morphology, during the drilling operation, the chips were collected for each hole in order to know and relate the type of chip formation with machining parameters and microstructure of the sample.

To analyse build-up edge, a microscope was used and photographs were snapped for the cutting tip of the drill bit to know and relate the formation of build-up edge with the machining parameters and physical properties of the sample material. Izod impact test was performed to measure the impact strength of the samples using impact testing machine. For each alloy, two specimens were tested for the repeatability.

3 Results and discussion

3.1 Microstructural examination

The optical micrographs of A6061T6, A5083 and LM6 samples are presented in Fig. 1a–c, respectively. In A6061T6 optical microstructure, Mg_2Si particles are identified at grain boundaries due to the precipitation formed from age hardening process. These particles prevent the dislocation of crystals and increase the hardness of the alloy [5]. Similarly, the Mg_2Si particles are also present at the grain boundaries of A5083 in large number which likewise resist the dislocations and improve the hardness and strength of the alloys. However, for the LM6 microstructure, the needle-like silicon particles can be seen which act as stress point and affect the hardness and strength of the alloy [14]. Correspondingly, the energy-dispersive spectra of A6061T6, A5083 and LM6 samples are presented in Fig. 1d, e, f, respectively.

Fig. 6 Chips collected for each experiment on A6061T6

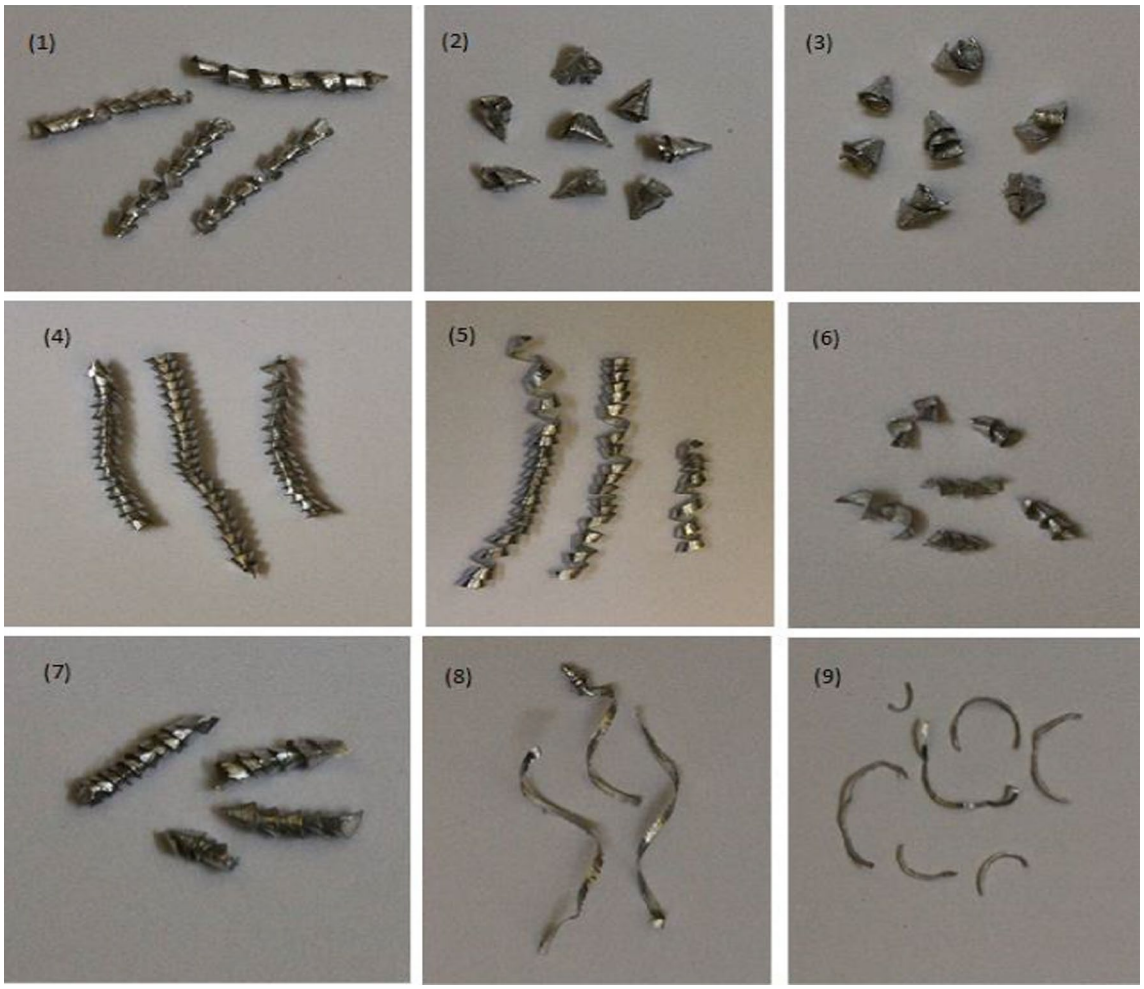

Fig. 7 Chips collected for each experiment on A5083

3.2 Hardness test analysis

The hardness test results are presented in Fig. 2. It can be observed that A5083 alloy bears the maximum hardness (81VHN) even though the Si content is very low (0.01wt %) in this alloy. This behaviour may be because of the formation of Mg_2Si phase in soft aluminium matrix [15]. Since the silicon and magnesium content is very low in A6061T6 alloy, the microstructure is primarily composed of aluminium grains with few Mg_2Si particles due to which the hardness is quite low. The presence of magnesium in A5083 gives strength to base alloy, and the hardness is comparatively high than A6061T6; this could be linked to the formation of Mg_2Si intermetallic.

3.3 Impact test

The impact test results from Fig. 3 show that the A5083 sample absorbed the maximum energy than the other two samples. This is due to the presence of Mg in the matrix which forms Mg_2Si particles, uniformly distributed at the grain boundaries. For the A6061T6, the impact strength is lower than A5083 because the distribution and formation of the Mg_2Si particles were not evenly distributed. Similarly, the impact strength in LM6 was found to be very low because of the needle-like silicon particles which act as stress risers and reduce the strength of the alloy.

3.4 Surface roughness

The surface roughness for holes drilled from all the samples with different drilling parameters is presented in Table 3 as plotted in Fig. 4. The surface roughness results showed that the average roughness values are different

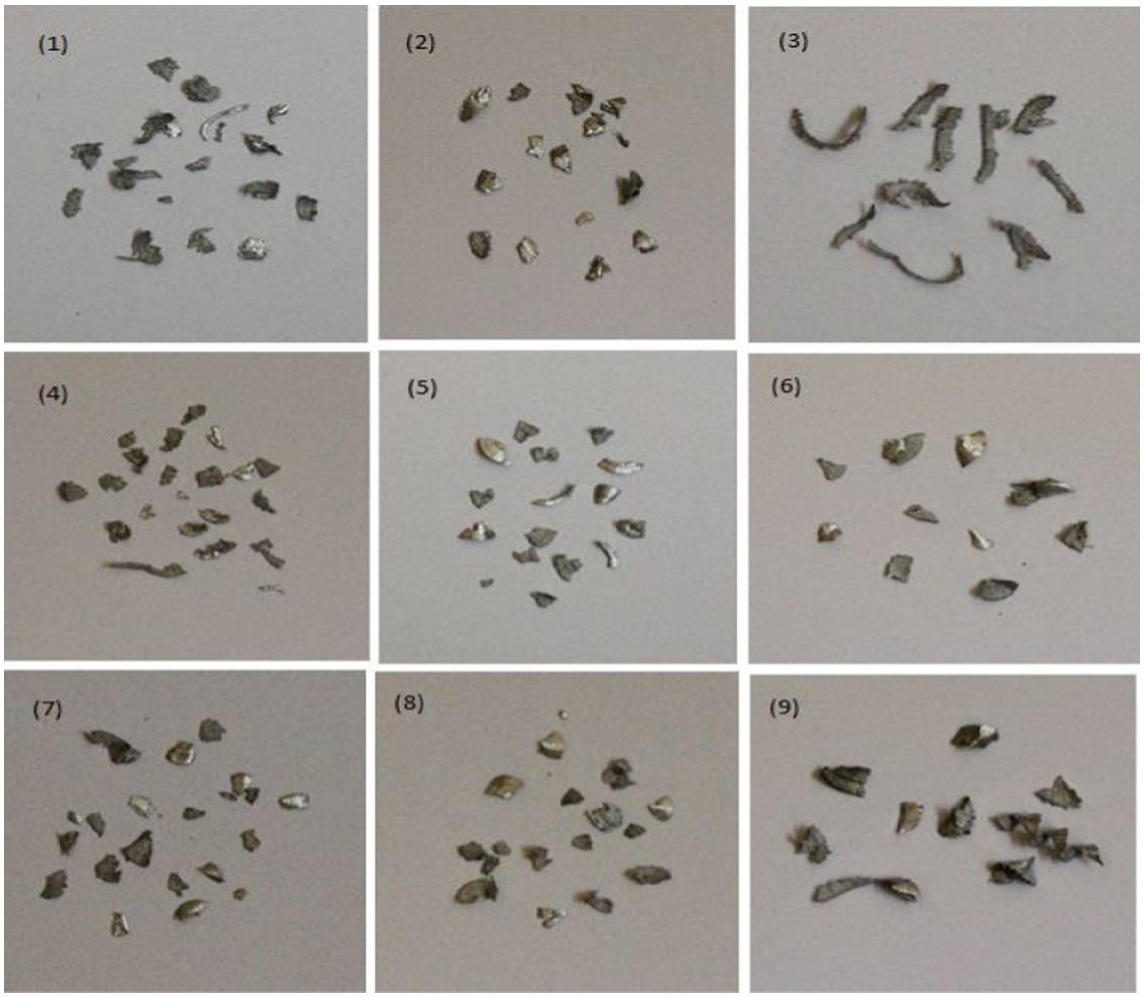

Fig. 8 Chips collected for each experiment on LM6

for all the three samples and the drilling parameters. Test results revealed that the soft ductile aluminium alloys exhibit more surface finish than the hard–brittle aluminium alloys [16]. LM6 and A6061T6 have the minimum roughness values for 3000 rpm spindle speed and 0.15 mm/rev feed rate. This is in good agreement with the fact that surface roughness improves with the increasing spindle speed [17, 18].

3.5 Burr formation

Figure 5 shows the plots for burr heights for each sample for different drilling parameters. The formation of burrs is related to both the material properties and the drilling parameters [19]. A major cause of burrs at the exit of the hole is extruding action of the drill bit [18]. The material ductility is also another reason for the burrs formed at the exit hole. From the graph, the height of burrs is maximum for A6061 T6 alloy due to its high ductility. For A5083 alloy and LM6, the burr height is reasonably low due to the presence of hard intermetallic Mg_2Si and silicon needles.

3.6 Chip morphology

The chips collected from A6061T6, A5083 and LM6 samples are shown in Figs. 6, 7 and 8, respectively. The chip shape and microstructure constitute a good indicator of the deformation having occurred during the machining process. The chip formation mode depends on the workpiece material, the tool geometry and the cutting conditions. A

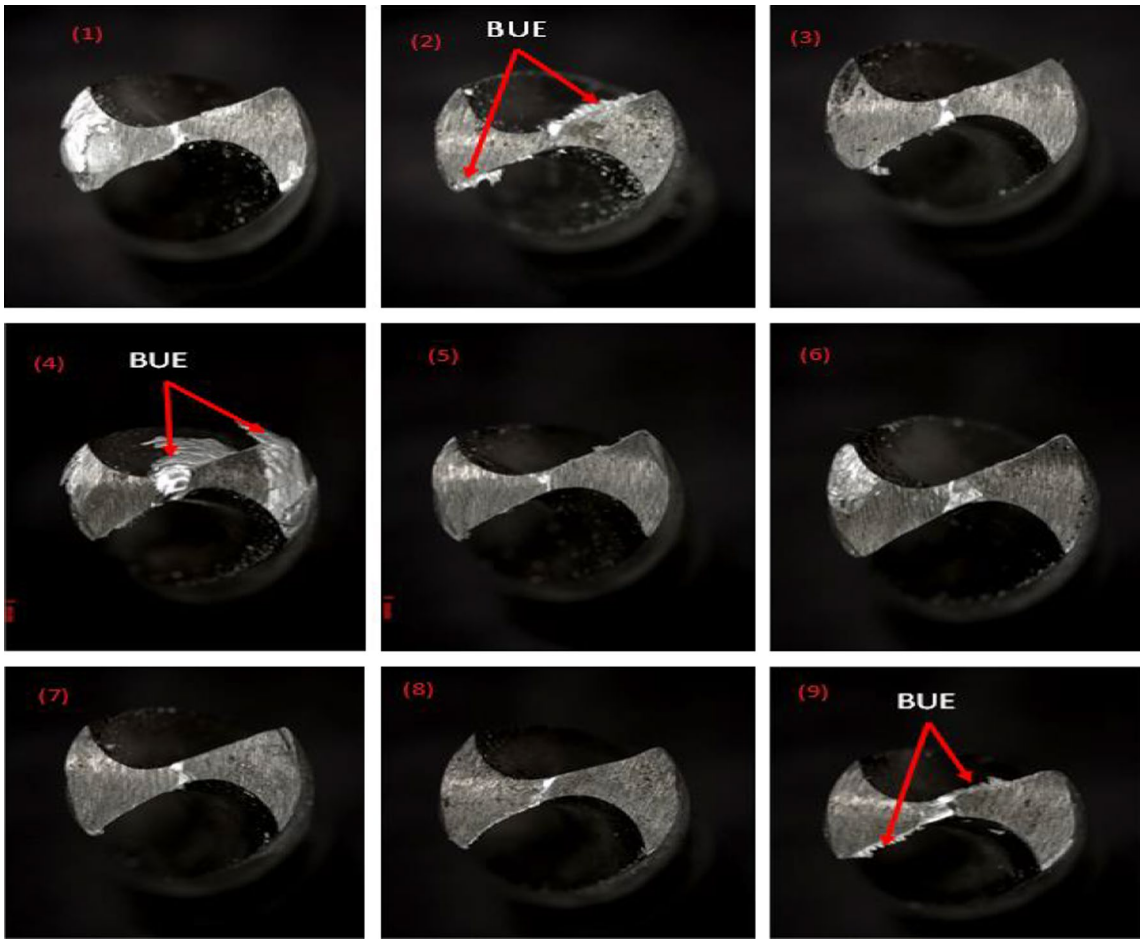

Fig. 9 Build-up formation for A6061T6

small and segmented chip is preferable when cutting metals. Similar to burr height and surface roughness, chip segmentation is also a function of material properties and the drilling parameters [20]. The chips formed from drilling of A6061T6 are continuous except for experiment no. 3. This is attributed to the proper feed rate and spindle speed which led to shearing of the chip that ultimately broke the chips in small fragments. Similar observation can be seen for A5083 alloy in which except experiment no. 2, the chips formed for rest of the experiments are continuous. And for LM6 that contains high silicon, the chips are mostly broken for all the experiments due to the brittleness and the chip thickness cannot support the shearing stresses and breaks [21].

3.7 Build-up edge (BUE)

Build-up edge is the mechanical adhering of soft material on the hard cutting edge due to the maximum forces involved in cutting action of material and the cutting edge [22]. BUE is detrimental to the surface finish and tool life. For A6061T6 and A5083 alloys, there is almost negligible BUE for each experiment. This is due to the moderate forces involved in cutting action of the material. But during the drilling of LM6, the cutting forces are high which generates heat at the cutting interface and the soft aluminium reaches near to melting and becomes mechanically weld with the cutting edge. This can be observed for all the experiments on LM6. The build-up formation on tool edge is shown in Figs. 9, 10 and 11 for A6061T6, A5083 and LM6, respectively.

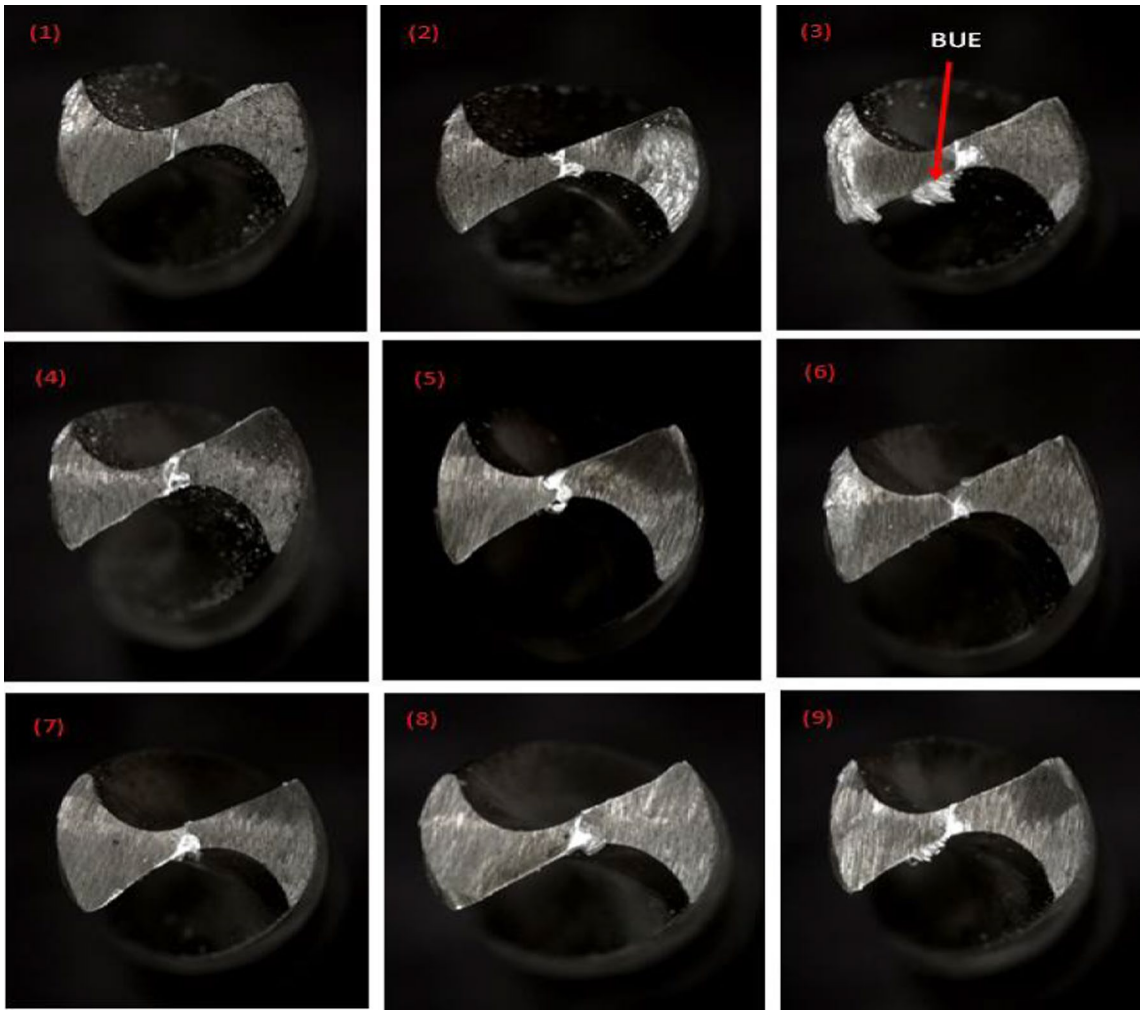

Fig. 10 Build-up formation for A5083

4 Conclusions

Considering the surface roughness, chip morphology, burr formation and build-up edge, the optimum drilling parameters for each alloy were established for surface roughness and burr height. Due to heat treatment of A6061, the surface roughness of A6061T6 was found minimum to be 3.8 µm; a feed rate of 0.15 mm/rev at a drilling spindle speed of 3000 rpm was found optimum without a build-up edge. Also, A5083 alloy with the minimum surface roughness of 4.9 µm could be drilled at an optimum feed rate of 0.15 mm/rev at a spindle speed of 1000 rpm without build-up edge. The optimum drilling spindle speed and feed rate values for A606T6 and LM6 are the same. However, the minimum surface roughness of LM6 was 4.2 µm with formation of minor build-up edge.

A minimum burr height of 0.7 mm was produced in drilling A6061T6 at an optimum drilling spindle speed of 1000 rpm and feed rate of 0.05 mm/rev with broken chip without a build-up edge. A minimum burr height of 0.1 mm was formed in A5083 at an optimum drilling spindle speed of 2000 rpm and feed rate of 0.1 mm/rev with broken chip without a build-up edge. A minimum burr height of 0.1 mm was also produced in LM6 with the same optimum drilling spindle speed and feed rate values in A606T6, but chip morphology in LM6 revealed a fine broken chip with minor build-up edge. However, for the future work, the same procedure is required to find optimum drilling parameters for smaller thickness than 30 mm of work part, since material thickness affects the holes quality. Also, the same procedure can be applied to find optimum drilling parameters by using carbide tools.

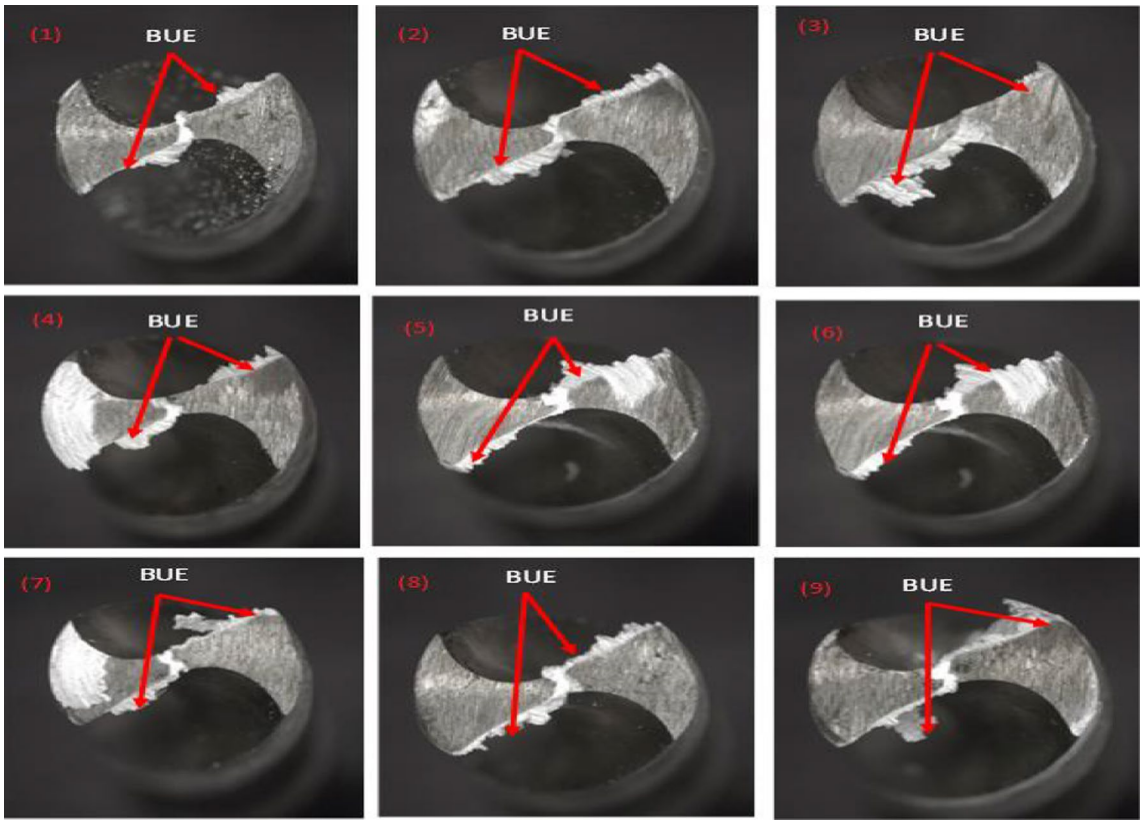

Fig. 11 Build-up formation for LM6

Acknowledgements The staff members in the Department of Materials, Manufacturing and Industrial Engineering, Faculty of Mechanical Engineering and Universiti Teknologi Malaysia are sincerely appreciated for their financial and technical support during and after this work. This work was partially supported by the Ministry of Higher Education of Malaysia (MOHE), Research Management Centre, Universiti Teknologi Malaysia, through GUP No: 20H28 and 06G32.

References

1. Madhu Kumar Y, Shankar U (2012) Evaluation of mechanical properties of aluminium alloy 6061-glass particulates reinforced metal matrix composites. Int J Mod Eng Res (IJMER) 2(5):3207–3209
2. Olohunde ST, Hafizi AM, Jamaliah I, Al-Bakoosh AA, Segun OO, Sadiq IO (2019) Corrosion resistance of aluminium-silicon hypereutectic alloy from scrap metal. J Bio Tribo Corros 5(2):41
3. Gale WF, Totemeier TC (2003) Smithells metals reference book. Butterworth-Heinemann, Oxford
4. Demir H, Gündüz S (2009) The effects of aging on machinability of 6061 aluminium alloy. Mater Des 30(5):1480–1483
5. Rao CP, Bhagyashekar M, Viswanath N (2014) Machining behavior of Al6061-fly ash composites. Procedia Mater Sci 5:1593–1602
6. Rajakumar S, Muralidharan C, Balasubramanian V (2010) Establishing empirical relationships to predict grain size and tensile strength of friction stir welded AA 6061-T6 aluminium alloy joints. Trans Nonferrous Met Soc China 20(10):1863–1872
7. Zhou C, Yang X, Luan G (2005) Fatigue properties of friction stir welds in Al 5083 alloy. Scr Mater 53(10):1187–1191
8. Gotoh K, Murakami K, Noda Y (2011) Fatigue crack growth behaviour of A5083 series aluminium alloys and their welded joints. J Mar Sci Technol 16(3):343
9. Sulaiman S, Sayuti M, Samin R (2008) Mechanical properties of the as-cast quartz particulate reinforced LM6 alloy matrix composites. J Mater Process Technol 201(1–3):731–735
10. Xu C, Jiang Q, Yang Y, Wang H, Wang J (2006) Effect of Nd on primary silicon and eutectic silicon in hypereutectic Al–Si alloy. J Alloys Compd 422(1):L1–L4
11. Ramulu M, Rao P, Kao H (2002) Drilling of (Al_2O_3) p/6061 metal matrix composites. J Mater Process Technol 124(1):244–254
12. Sadiq TO, Daud LM, Idris J (2018) Investigation of microstructure and mechanical properties of A335 P11 main steam pipe in Stesen Janaelektrik Jambatan Connaught Power Plant, Malaysia. Trans Indian Inst Met 71(10):2527–2540
13. Buha J, Lumley R, Crosky A, Hono K (2007) Secondary precipitation in an Al–Mg–Si–Cu alloy. Acta Mater 55(9):3015–3024
14. Pengfei X, Bo G, Zhuang Y, Kaihua L, Ganfeng T (2010) Effect of erbium on properties and microstructure of Al–Si eutectic alloy. J Rare Earths 28(6):927–930
15. Pezda J (2014) The effect of the T6 heat treatment on hardness and microstructure of the EN AC-AlSi12CuNiMg alloy. Metalurgija 53(1):63–66
16. Behera R, Sutradhar G (2012) Machinability of LM6/SICP metal matrix composites with tungsten carbide cutting tool inserts. ARPN J Eng Appl Sci 7(2):216–221

17. Senapati AK, Brata Mohanty S (2014) A review on the effect of process parameters on different output parameters during machining of several materials. Int J Eng Sci Res Technol 3(3):1499–1508
18. Sadiq TO, Olawore SA, Idris J (2018) Energy consideration in machining titanium alloys with a low carbon manufacturing requirements: a critical review. Int J Eng Res Afr 35:89–107
19. Barani A, Amini S, Paktinat H, Tehrani AF (2014) Built-up edge investigation in vibration drilling of Al 2024-T6. Ultrasonics 54(5):1300–1310
20. Songmene V, Djebara A, Zaghbani I, Kouam J, Khettabi R (2011) Machining and machinability of aluminum alloys. In: Kvackaj T (ed) Aluminium alloys, theory and applications. IntechOpen. https://doi.org/10.5772/14888
21. Dwivedi D, Sharma A, Rajan T (2008) Machining of LM13 and LM28 cast aluminium alloys: part I. J Mater Process Technol 196(1):197–204
22. Taskesen A, Kutukde K (2013) Analysis and optimization of drilling parameters for tool wear and hole dimensional accuracy in B4C reinforced Al-alloy. Trans Nonferrous Met Soc China 23(9):2524–2536